CHAPTER IV

STRENGTH PROPERTIES

Having investigated the nature of Vickers-produced cracks in cattle bone materials, we will now use them as strength controlling cracks. Accordingly a two-step procedure forms the basis of the test used in this study of strength properties of cattle bone materials : the specimen is first loaded with a Vickers indenter to introduce a median / radial crack into the surface, and is subsequently taken to failure in a four-point bending test. This procedure, together with a very current strength theory (27) in which the influences of residual contact stresses as well as the microstructural driving stresses, are explicitly recognized will be used to establish a mean for evaluating cattle bone materials in stress-bearing applications.

4.1 Theory of Failure from Radial Crack Under Equilibrium Fracture Conditions

A schematic diagram of the indentation failure sequence is given in Fig. 4.1. Accordingly for equilibrium pennylike cracks of characteristic subsequently subjected to an applied tensile stress σ_a, the stress intensity factor K is as the form

$$K = K_a + K_r \tag{4.1}$$

wher K_a and K_r represent corresponding contributions to the net crack driving force from the applied loading and the residual contact fields. An expression of K_a corresponding to the radial crack system
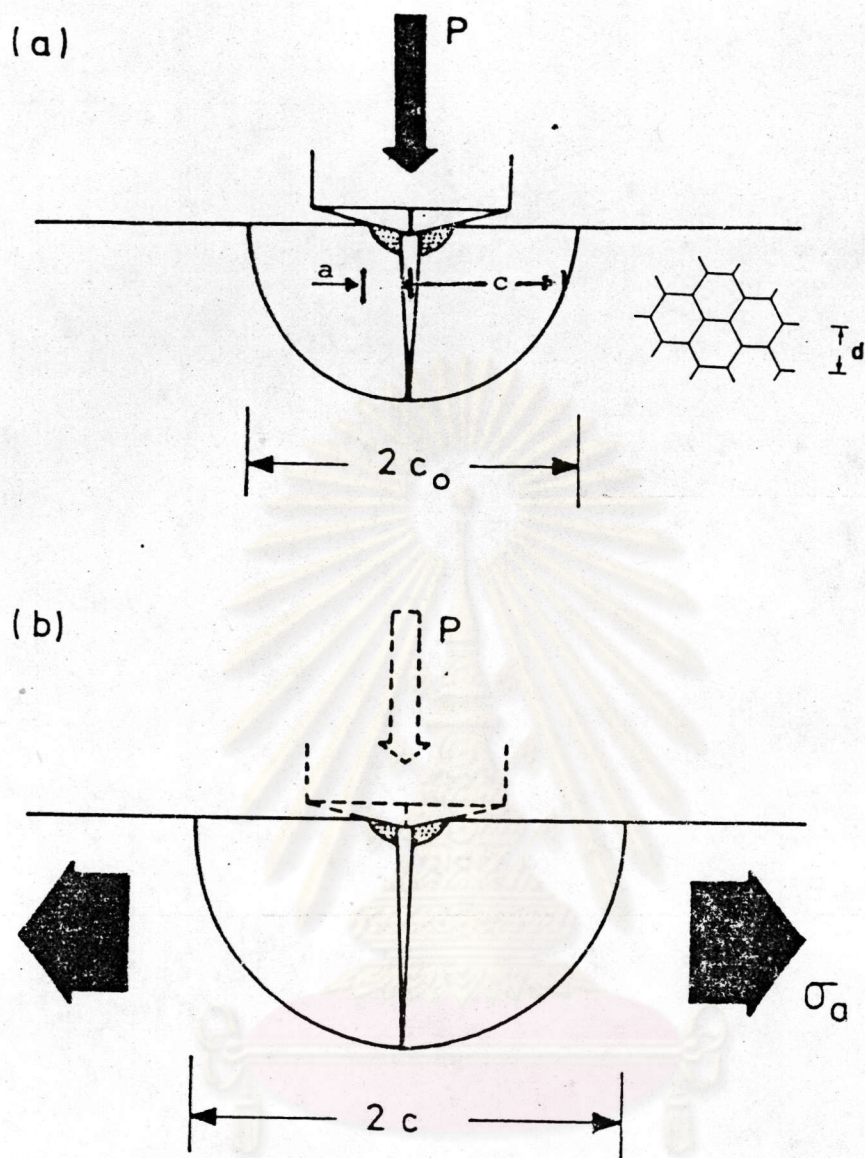
Fig. 4.1 Schematic of indentation / strength sequence.

(a) Vickers indenter, peak load P, generates radial

crack characteristic dimension c (value c immediately

after contact, with post - endentation extends to c_o

if exposed to reactive environment). Dimension a, c,

and d characterize scale of central hardness impression,

radial crack, and microstructure "grains", respectively.

(b) Tensile field σ_a combines with residual contact

field to drive crack to failure configuration.

oriented normal to the applied tensile direction is

$$K_a = \psi \sigma_a c^{1/2} \tag{4.2}$$

where ψ is a dimentionless crack - geometry constant. An expression for the residual stress intensity factor is

$$K_r = \chi_r P/c^{3/2} \tag{4.3}$$

where χ_r is a dimentionless constant which characterize the level of the residual contact field and its magnitude depends on the E/H ratio

$$\chi_r = \xi^R (E/H)^{1/2} \tag{4.4}$$

where ξ^R is a material - independent constant for Vickers - produced median / ridial cracks (Sect. 3.1.3).

Thus the criterion for equilibrium fracture may be written (Sect. 3.1)

$$K = \psi \sigma_a c^{1/2} + \chi_r P/c^{3/2} = K_c' \tag{4.5}$$

Here the effective toughness K_c' is used for the term on the right side of Eq. (4.1) in order to allow for the dependence of toughness parameter on the ratio of crack size to grain size d. According to Cook et al. (27) K_c' can be expressed as

$$K_c' = K_c^\infty - K_m$$
$$= K_c^\infty - \mu Q/c^{3/2} \tag{4.6}$$

where K_c^∞ is the macroscopically determined toughness appropriate to the material response with crack size large compared to its grain size and the quantity μQ has the interpretation of a microstructural driving force.

Eqs. (4.5) and (4.6) may now be combined to give the stress intensity factor for equilibrium indentation cracks,

$$K = K_a + K_r + K_m$$
$$= \Psi \sigma_a c^{1/2} + (X_r P + \mu Q)/c^{3/2} = K_c^{\infty} \qquad (4.7)$$

Eqs. (4.7) may be solved for applied stress σ_a as a function of crack size,

$$\sigma_a = (K_c^{\infty}/\Psi c^{1/2}) [1 - (X_r P + \mu Q)/K_c^{\infty} c^{3/2}] \qquad (4.8)$$

The strength / load characteristics are obtained by determining the condition for instability in the function $\sigma_a(c)$ from Eq. (4.8). By virtue of the inverse dependence on c of the second term in Eq. (4.8) radial crack grows stably at its final stages of evolution, producing the precursor growth characteristic before failure.

In the limit of large cracks, i. e. $X_r P \gg \mu Q$, we may approximate Eq. (4.8) as

$$\sigma_a = (K_c^{\infty}/\Psi c^{1/2}) [1 - X_r P/K_c^{\infty} c^{3/2}] \qquad (4.9)$$

which passes through a maximum at

$$\sigma_m^P = 3 K_c^{\infty}/4\Psi c_m^{1/2} \qquad (4.10)$$

$$c_m = (4X_r P/K_c^{\infty})^{2/3} \qquad (4.11)$$

It is noted that the superscript P is used to denote an indentation - controlled region of behaviour. A plot of the function $\sigma_a(c)$ in Eq. (4.9) is shown in Fig. 4.2 for nonzero and zero X_r. For an initial crack size c_o' the two cases represented have totally different failure paths. Path 1 is the Griffith limit in which failure occurs spontaneously at $\sigma_a = \sigma_o = K_c/(\Psi c_o')^{1/2}$. Path 2 is
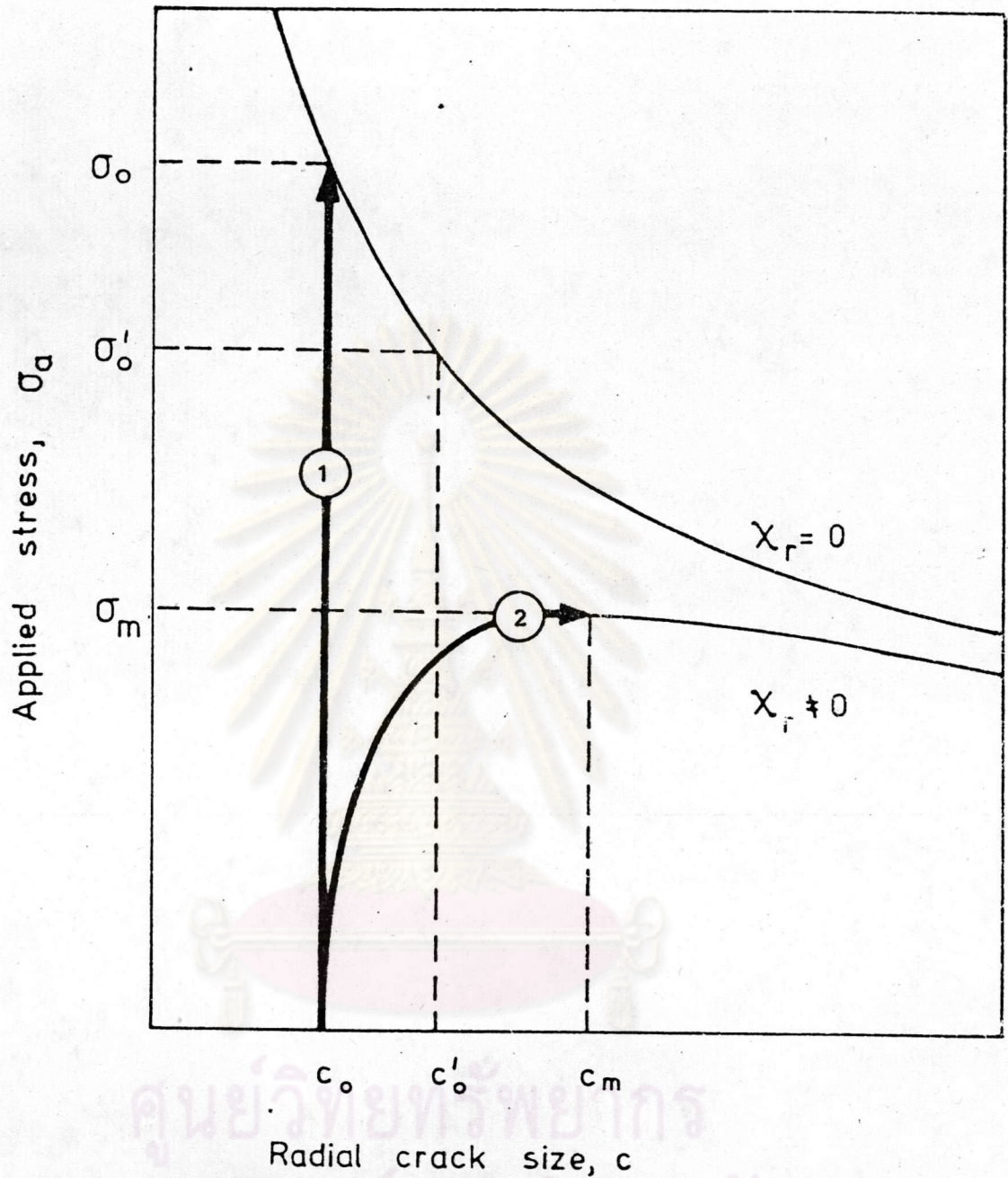
Fig. 4.2 Plot of function δ_a (c) in Eq. (4.9) for radial cracks with and without residual contact stress. Curve 1 and 2 indicate respectively paths to fail under equilibrium fracture conditions.

distinguished by a stage of precursor radial expansion, from c_o' to c_m, prior to the system reaches an instability at $\sigma_a = \sigma_m^P$, which defines the inert strength. Eq.(4.10)thereby give the inert, residual -stress - sensitive strength and the substitation of Eq.(4.11)into (4.10)gives

$$\sigma_m^P = 3 \, K_c^\infty{}^{4/3}/4^{4/3} \, \psi \, (\chi_r P)^{1/3} \tag{4.12}$$

Now in the opposite limit of small cracks, i. e. $\chi_r P \ll \mu Q$, a solution of identical form to Eq. (4.10) may be written,

$$\sigma_m^Q = 3 \, K_c^\infty{}^{4/3}/4^{4/3} \, \psi \, (\mu Q)^{1/3} \tag{4.13}$$

with the superscript Q denoting a microstructural - controlled region. Fig 4.3 shows Eqs. (4.12) and (4.13) as straight lines in (logarithmic) σ_m (P) coordinates. The intersection point at $P = P^*$ in this plot conveniently delineates the two regions of behaviour. It is noted that be equating σ_m^P and σ_m^Q we obtain

$$\chi_r P^* = \mu Q \tag{4.14}$$

where P^* is an analogous load which incorporates the microstructural driving force.

Substituting Eq. (4.14) for μQ into Eq. (4.8) gives the general strength / load characteristics as

$$\sigma_a = (K_c^\infty/\psi c^{1/2}) \, [1 - \chi_r(P + P^*) / K_c^\infty c^{3/2}] \tag{4.15}$$

which passes through a maximum at

$$\sigma_m = 3 \, K_c^\infty{}^{4/3}/4^{4/3} \, \psi \, \chi_r^{1/3} \, (P + P^*)^{1/3} \tag{4.16}$$

$$c_m = [4\chi_r (P + P^*)/K_c^\infty]^{2/3} \tag{4.17}$$

The Eq. (4.16) gives the corresponding critical applied stress which defines strength and Eq. (4.17) gives the critical crack size at
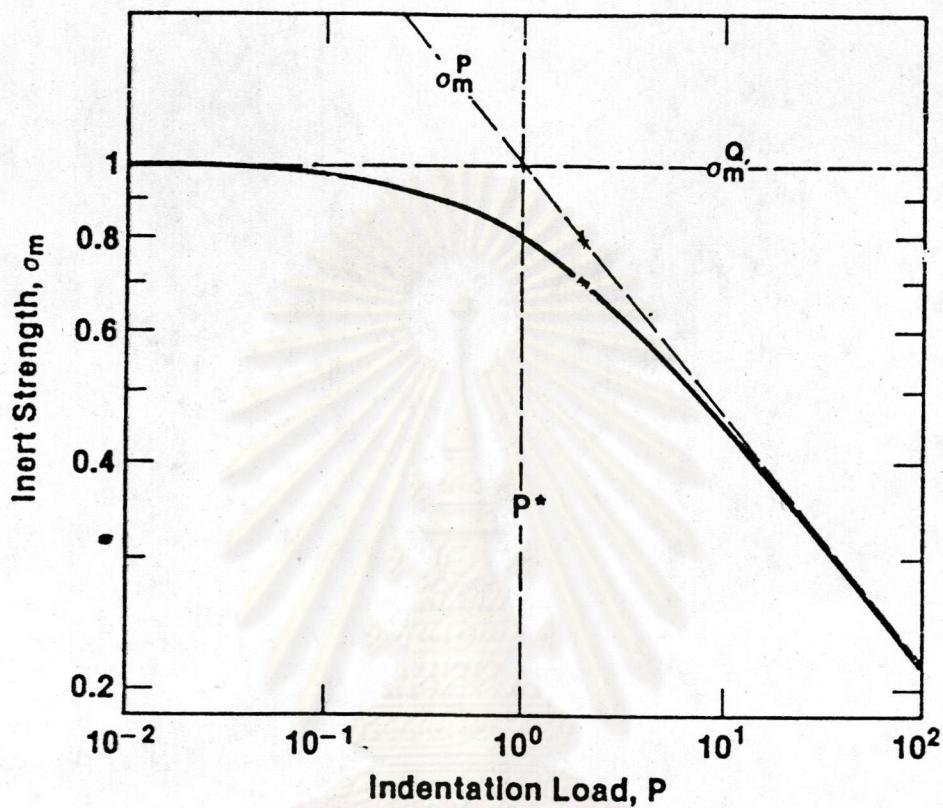
Fig. 4.3 Normalized plots of strength vs indentation load.

Dashed broken lines asymptotic to this curve are

limiting solutions (Eqs. 4.12 and 4.13). Intersection

point between latter two solutions conveniently

distinguishes indentation and microstructure - controlled

regions of behavior.

instability. A plot of this general function is included in Fig. 4.3.

4.2 Basic Experimental Techniques

The four - point bending test was selected as a means for measuring failure stresses of the indented specimens. Such test obviated the need for uniaxial tensile testing, with its attendant gripping and alignment problems. Thus the specimens and the four - point bending fixture used in this study were designed so that precise measurements of failure stresses could be obtained. The four - point bending fixture was chosen to be constructed suitable for specimens in the form of rectangular shape. According to ASTM specifications (31) (i) the separation of the loading edges should not be less than 19 mm and at least three times the thickness of the specimen, (ii) the moment arm or separation of adjacent support and loading edges should be greater than the width of the specimen and at least four times the thickness of the specimen. Thus the specimens were prepared in the form of bars of dimension 63 mm x 7 mm x 5 mm and 60 mm x 6 mm x 5 mm at sintering temperature 1250° c and 1345° c, respectively, and the four - point bending fixture was constructed and set up as shown in Figs. 4.4 and 4.5, with an inner span of 19 mm and an outer span of 60 mm. The loading was obtained by connecting the loading fixture into the underside of the crosshead of a Shimudzu testing machine and seating the loading support on a compression load cell (maximum load 100 KN). The test fixture was designed to allow for the symmetrical alignment of the axes of the loading fixture and loading support.

The bar specimen was indented midway along its length (Sect. 3.2), with symmetrical alignment so as to produce radial cracks

Fig. 4.4   Illustration of   components of the four – point bending

fixture designed and constructed in accordance with
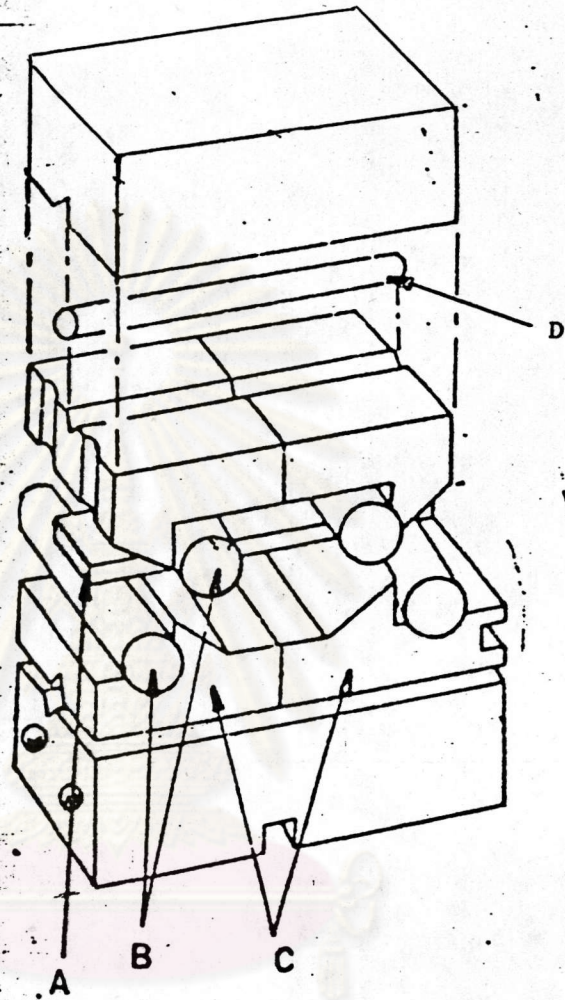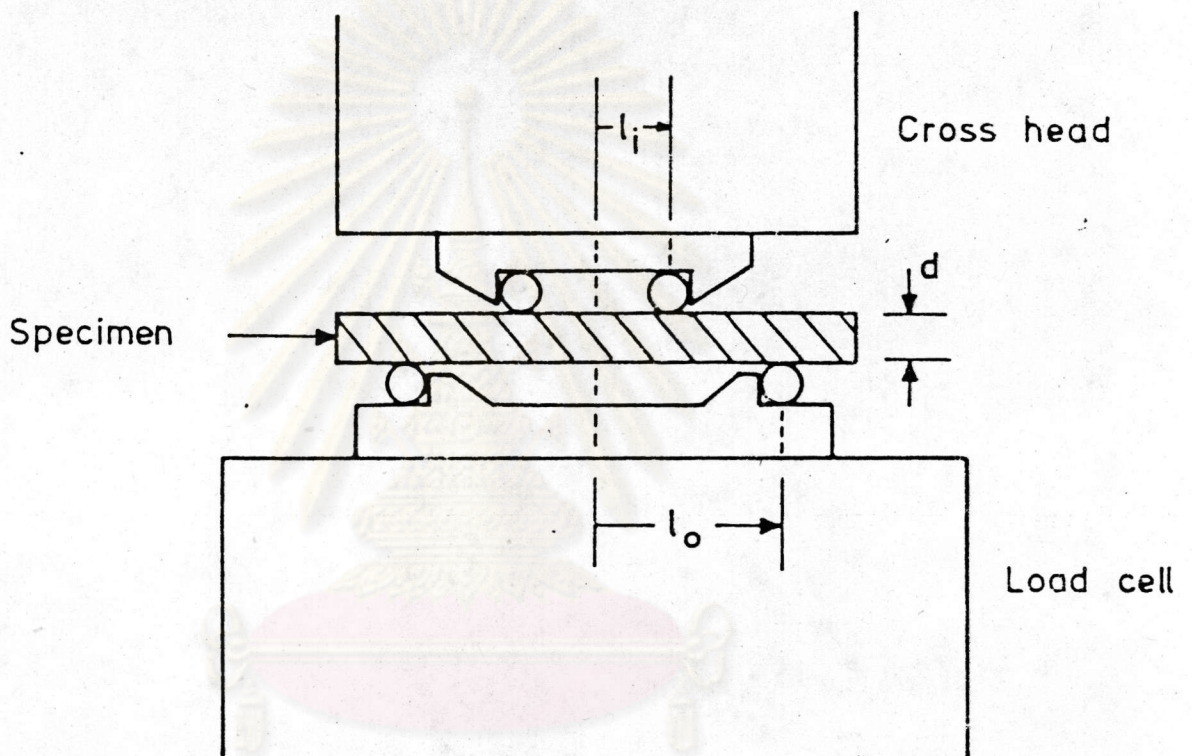
ASTM specifications.

Fig. 4.5   Schematic of bend fixture. (a) Specimen at A is

loaded via hardened steel rollers, B. Independently

rotatable hardened steel ways (lower pair indicated

at C) support the rollers and are free to pivot

about bearings, one of which is indicated at D. ;

Cross head

Specimen

l_i

d

l_o

Load cell

(b) Schematic of experimental setup for uniaxial strength testing of bar specimens.

perpendicular to the subsequent applied tension. The indented
specimen was then mounted on the loading support with the indented
face on the tenside side. The specimens were finally loaded to
failure at preselected constant - displacement rate, with the applied
load recorded on a chart recorder. The failure stresses (strengths)
were evaluated using simple beam theory (30):

$$\sigma = 3 \, (l_o - l_i) \, Q/bd^2 \qquad\qquad (4.18)$$

where Q is the failure load, b the specimen width, d the specimen
thickness, l_o and l_i the outer and inner half - spans of the four-
point bending fixture, respectively.

4.3 Experiment

4.3.1 Exploratory Tests

(a) Effect of Stress Rates on Strength

It has been indicated in Sect. 3.3.3 that the
cattle bone material is highly susceptible to moisture - assisted
slow crack growth. In order to obtain its equilibrium strength data,
the effect of moisture - assisted slow crack growth must therefore be
minimized during strength tests. This may be done by performing
strength tests in oil. Furthermore a suitable stress rate should
be selected : if the stress rate is too low, an appreciable slow
crack growth effect will occur ; on the other hand if the stress rate
is too high, the dynamic effect will take place. Thus in order to be
able to select the most appropriate stress rate, which make the oil
environment being effectively inert, strengths of the indented
specimens were measured as a function of stress rate. A fixed

indentation schedule was adopted so that a consistent starting crack size was produced for all specimens : each bar was indented in air at its center with a Vickers indenter at a peak load of P = 10 N and was left in air for more than 60 min to allow for saturation of post - indentation slow crack growth (Sect. 3.3.3). Immediately before commencing four - point bending tests at a prescribed crosshead speed (Sect. 4.2), the indentation site was covered with a drop of immersion oil. Fig. 4.6 shows strength behaviour of the 10 N indented
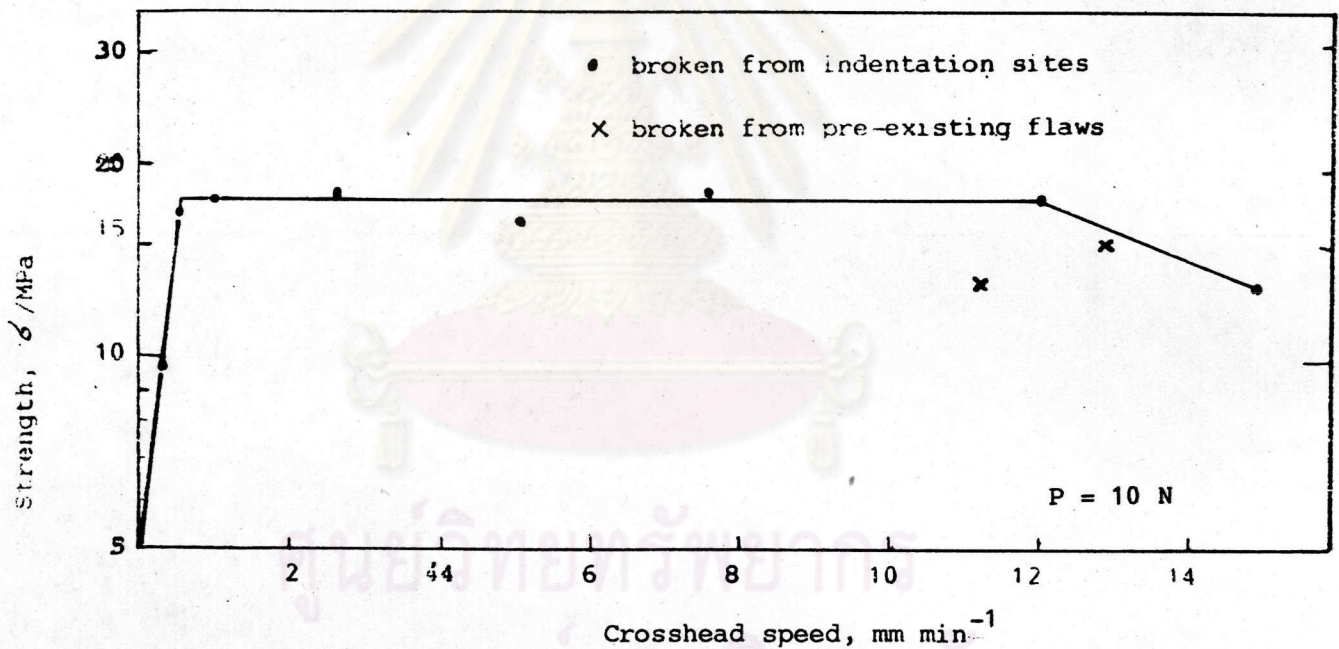

Fig. 4.6   Failure stress as a function of corsshead speed of the crosshead testing machine. Each data point represents the mean value strength of at least 5 tests.

cattle bone material as a function of crosshead speed. Each data point represents the mean and standard deviation (at least 5 specimens) at each crosshead speed.

The results summarized in Fig. 4.6 demonstrate that an appreciable moisture - assisted slow crack growth takes place at stress rates corresponding to crosshead speeds below 1.0 mm min^{-1} and an appreciable dynamical effect at stress rates corresponding to crosshead speed above 12.0 mm min^{-1}. Strengths tend to be a plateau at stress rates corresponding to crosshead speed between 1.0 and 12.0 mm min^{-1}. Thus this range of stress rates tend to be the most appropriate to be used for inert strength tests. In the present work the crosshead speed of 2.0 mm min^{-1} was chosen to deliver stress in the inert strength tests.

(b) Effect of Surface Finishing on Strength

It has been found in a wide range of ceramics that the strengths for as - machined surfaces were considerably higher, by 50 %, than those for as - polished surfaces (38). The results were interpreted in terms of a residual compressive stress layer in the initial machined surface. Such a surface - stress layer will complicate the strength analysis and will lead to significant errors in the evaluation of material parameters if it is not taken into account properly. Therefore to ensure that cattle bone materials used in the strength test runs free of any pre- existing surface stresses, preliminary tests were made on the following surface finished specimens : 1200 mesh SiC paper ground surfaces, 2.5 μm diamond paste polished surfaces, 1 μm diamond paste polished surfaces.

Similar to the exploratory test of stress rates on strength, a fixed indentation schedule, in which a peak load of P = 10 N was used to introduce a consistent starting crack size into all specimen surfaces, was adopted (Sect. 4.3 (a)). The indented bars were subsequently broken in the four - point bending tests at a crosshead speed of 2 mm min^{-1} (Sect. 4.2).

The results of the strength tests are plotted in Fig. 4.7. Each data point represents the mean and standard deviation of at least three specimens broken at the indentation sites.

The systematic decrease in strength from $21.2^{\pm}2.0$ MPa to $14.3^{\pm}0.03$ MPa as the surface finishing changes from 1200 mesh SiC paper ground surface to 1 μm diamond paste polished surface demonstates that residual compressive stresses have been introduced into the surfaces of cattle bone material during grinding with SiC papers and such compressive stress layers were removed with progressive removal of grinding damage layer by a polishing procedure. Thus it can be concluded from these data that grinding damages do strengthen cattle bone material. However, as we wish to evaluate toughness parameter of cattle bone material from the indentation-controlled strength data, the surface of specimens used in such tests are therefore polished down to 1 μm diamond paste with considerable time to ensure that no pre - existing surface - stressed states exist.
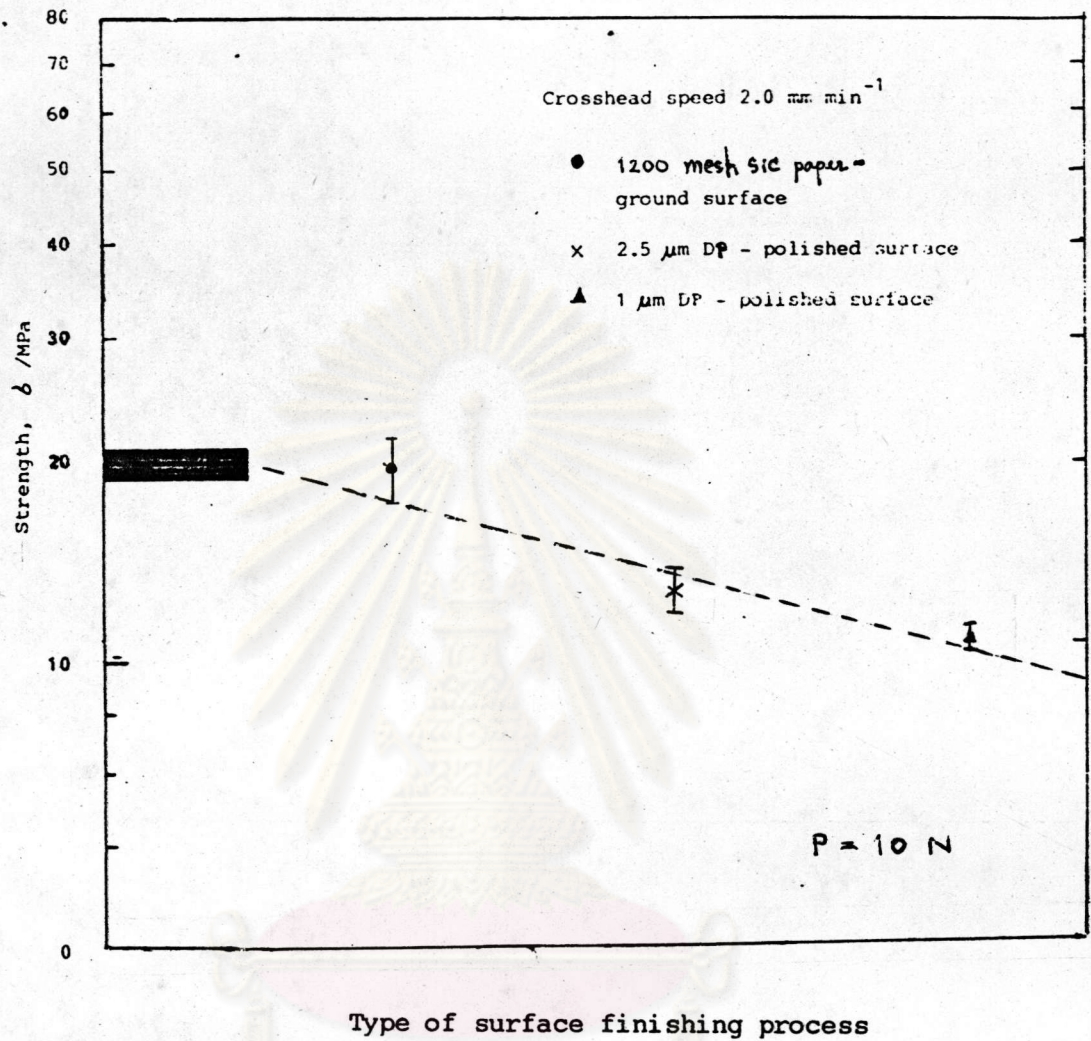
Type of surface finishing process

Fig. 4.7   Equilibrium failure stress related with type of sarface finishing process for cattle bone material. The shaded band is "as-polished" strength. All specimens were broken from indentation sites. Error bars are standard deviations of 3 specimens broken form the indentation site.

4.3.2 Procedure and Results

With the data obtained in the exploratory tests

(Sect. 4.3.1), we are now in a position to run a proper indentation -

controlled strength tests since such data provide a means to prepare

the most suitable surface finish of test materials (1 μm diamond

paste finish) and to choose the most appropriate cross head speed

(2.0 mm min^{-1}) used in delivering stresses onto the indented

specimens in oil environment. Moreover, in order to be able to

deduce the microstructural effect on strengths of cattle bone

materials, two sets of cattle bone materials sintered at 1250° C

and 1345° C were chosen as test materials. These were specimens of

minimum (0.6 μm) grian sizes and maximum (6 μm) grain sizes that

could be prepared without the occurrence of second phase material

(Sect. 2.2.2).

A series of strength tests was run for the two sets

of specimens over the widest possible range of indentation loads

(Sect. 3.2). Each test piece was polished with a series of grit

sizes of Si C papers (800, 1000, 1200 mesh) and diamond pastes (2.5,

1 μm). By this means, smooth surfaces 1 μm diamond paste finish

were obtained. When the polishing process was completed, each

specimen was indented midway along its length of its prospective

tensile surface with a Vickers indenter at a prescribed peak load

using standard loading facilities (Sect. 3.2) and with symmetrical

alignment so as to produce radial cracks perpendicular to the

subsequent applied tension. The indented specimens were then taken

to failure in four-point bending and simple beam theory was used to

evaluate the corresponding tensile stress on the crack (Sect. 4.2).

The average interval between mdentation and bending was about 2 hrs, during such time the cracks were exposed to air to allow for saturation of postindentation slow crack growth. During the bend test, the indented sites were covered with a drop of immersion oil and a crosshead speed of 2 mm min^{-1} was used so that fracture occurs under essentially equilibrium fracture conditions (Sect. 4.3.1 (a)). All broken specimens were examined optically to confirm that failure had occurred from the indentation site; a few specimens broken from other ovigin s (more frequently at relatively low indentation loads where pre-existing flaws dominate), and these were duly deleted from the data accumulation. Logarithmic plots of the measured strength as a function of indentation load are shown in Fig. 4.8. Each data point represents the mean and standard deviation of three specimens breaking from indentation crack at a precribed load. The inclined solid lines are least - squares best fits to the mean value of quantity of $6P^{1/3}$ computed over all specimens 3 containing relatively high load indentations for each set of specimens. At low loads, a strength plateau occurs, indicating a region of behaviour which is microstructure controlled.

An additional method of recording crack configuration near the point of failure was also used in the strength test. This involved placing additional identical indentations along the longitudinal center-line in the tensile face, loading the bar to faiilure and finally examining the indentations which had survived each bar failure. Accordingly three 10 N indentations were made within the inner - span region of the cattle bone bars, with each indentation spaced 2 mm from its neighbours to avoid intersetion effects. Such
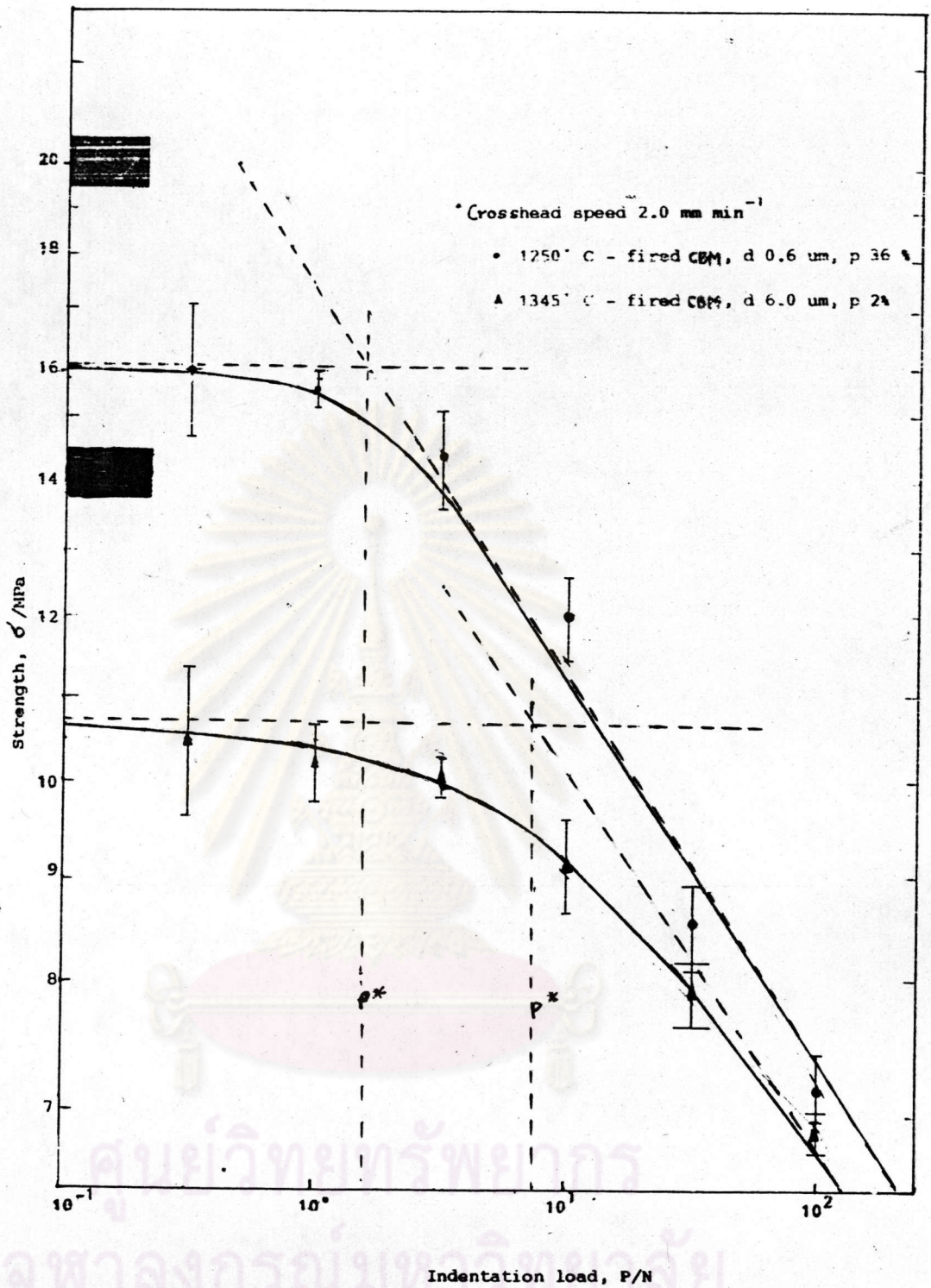
Fig. 4.8   Equilibrium failure stress as a function of indentation
load for the polished specimeans, (CBM = cattle bone
material, d = grain size, p = porosity). The upper shaded
band is as-polished strength of 0.6 μm grain specimen and
the lower one is as-polished strength of 6.0 μm grain
specimen. Error bars are standard deviations of
3 specimens broken from the indentation site.

specimens were then loaded to failure in four-point bending. From the investigations show that fracture originated from the central indentation whereas other two indentations survived. Also the radial cracks of the remaining indentations which perpendicular to the tensile bend oxis areseen to be longer about 50 % than those parallel to the tensile bend axis. This indicates that the radial cracks perpendicular to the tensile bend axis experienced the applied tension and extended stably without failure whereas those parallel to the tensile bend axis were unaffected by the bending. This evidence of stable crack growth demonstrates the importance of taken into account the influence of residual contact stresses, which accompany the indentation crack of cattle bone material, into strength analysis. In addition, the radial cracks perpendicular to the tensile bend axis must have been taken very close to the instability configuration , and accordingly provide a measure of maximum crack size c_m before failure. The value of c_m is useful in the evaluation of some fracture parameters, e.g. the crack - velocity exponent (33).

4.4 Discussion

The toughness K_c which is an important fracture parameter for ceramics may be evaluated from direct indentation - crack measurement data and is obtained to be 0.07 MPa.m$^{1/2}$ for cattle bone material. However, the exposure of the newly formed fracture of the cattle bone material to a reactive environment (Sect. 3.3.3) may result in considerable extension by slow crack growth, making the value determined somewhat less than the true K_c. This error is difficult to avoid. The indentation / strength method overcomes

the problem due to post - indentation slow crack growth. This is because the equilibrium strength of the indented flexural specimen is independent of the initial indentation crack size. Accordingly, the post - indentation slow crack growth has no consequence on the equilibrium strength.

From the investigation of the effect of surface finishing process, the result shown in Fig. 4.7 indicates that the material is less immune to strength degradation from post - preparation contact events when their surfaces are prepared with a relatively smooth finish, i. e. polishing down to very fine diamond paste. On the other hand, the grinding process finished with SiC paper lead to the presence of a surface compression layer which may be regarded as the cumulative manifestation of a vast number of related indentation events, such that neighboring residual contact fields show the overlapping. However, the compressive stress will generally leads to a greater complexity in crack response and the determination of the appropriate stress intensity factor for fracture mechanics analysis. Therefore, any pre-existing surface stress is preferably removed before an attempt to evaluate fracture parameters using controlled surface crack has been made.

The evidence of stable crack growth, which is appeared on the surviving intentations on the bar demonstrates that the simplistic Griffith concept of the residual stress-free crack, in which failure occurs spontaneously at some critical stress (See Fig. 4.2), is not applicable to the analysis of strength behaviour of cattle bone material containing indentation crack. Thus, the residual contact

stress has been incorporated in the fracture mechanics analysis in order to provide a reliable fracture parameter which can reflect the appropriate strength properties of cattle bone material.

In the conventional method, fracture mechanics measurements are made on large - scale crack specimens. In the indentation method the size of the cracks can be varied systematically via the indentation load, thereby allowing for controlled progression from macroscopic to microscopic domains. Accordingly the strength data of cattle bone materials as a function of indentation load reveal their strength as a function of crack size relative to grain size. The microstructural effect on their strength properties can thus be observed. From the result shown in Fig 4.8 (Sect. 4.3.2), the intersection point at $P = P^*$ conveniently delineats the two regions of behaviour : the indentation - controlled region in which the crack responsible for failure are large compared to grain size, and the microstructure - controlled region in which the strength - controlling crack is of the same order as the grain themselves. The deduced toughness which is used to describe equilibrium fracture processes in the indentation - controlled region will be represen- tative for the macroscopic toughness, K_c^∞. An expression for K_c^∞ can be obtained from Eqs. (4.10) and (4.11), making use of the difinition of X_r in Eqs. (4.4).

$$K_c^\infty = \eta_v^R \, (E/H)^{1/8} \, (\delta_m^P \, P^{1/3})^{3/4} \qquad (4.19)$$

where η_v^R is another nondimensional constant characteristic of the indenter geometry. Chantikul et al. (11) established a value,

$$n_v^R = (256 \, \gamma^3 \, \xi_v^R \, /27)^{1/4} = 0.59$$

for the standard Vickers indenter by calibrating indenter crack

strength data on ceramics of known toughness. Using Eq. (4.19), K_c

deduced for cattle bone material with 6.0 μm grain size and 0.6 μm

grain size are 0.18 and 0.20 MPa m$^{1/2}$, respecitively. When

microstructure effects are present, Eq. (4.19) retains its validity

only in the limiting region of large P.   Recalling Eq. (4.16),

we may expressed in the other two forms as

$$\sigma_m = \sigma_m^Q \, P^{*1/3} / (P+P^*)^{1/3}$$

$$= \sigma_m^P \, P^{1/3} / (P+P^*)^{1/3} \qquad (4.20)$$

It will be noted from Eq. (4.20) that of the three measurable material

constants σ_m^Q, $\sigma_m^P \, P^{1/3}$, and P^*, only two are required to provide a

unique determination of the strength characteristics in Fig. 4.8.

It becomes apparent that the macroscopically determined

toughness K_c^∞ is insufficient for describing strength properties at

the microstructural level. The strengths in the plateau region

are significantly lower than those obtained by extrapolations from

the high load, indentation - controlled region. In this study, the

coarser grain cattle bone material shows the relatively pronounced

plateau. Thus in the present experiments, it is the cattle bone

material sintered at 1250°C which by virtue of its finer microstruc-

ture, has the superior response in the low - loaded region. However,

the plateau strength themselves may constitute the most suitable

design parameters, not only because they relate directly to crack

behaviour in the domain of naturally occurring cracks but also

because of their insensitivity to extraneous contact - related events.

Finally, it is particular importance to point out that although the indentation cracks are artificially introduced entities, there is considerable evidence to demonstrate that they do indeed simulate the essential qualities of naturally occurring surface cracks in ceramic components (12). Therefore, the sharp - indentation / strength tests can be regarded as a representative model of the typical individual contact event encountered in practice of cattle bone materials (i. e. implanting into the living system). The results summarized in Fig. 4.8 serve to show how strength varies with the severity of the contact degradation occur. Eq. (4.15) allows for approximated prediction of strength degrading characteristics for cattle bone materials.